Immunomodulatory IL-23 receptor antagonist peptide nanocoatings for implant soft tissue healing

John A. Pizarek[a,b], Nicholas G. Fischer,*[a] and Conrado Aparicio*[a,c,d]

[a]MDRCBB-Minnesota Dental Research Center for Biomaterials and Biomechanics, University of Minnesota, 16-212 Moos Tower, 515 Delaware St. SE, Minneapolis, Minnesota 55455, USA

[b]United States Navy Dental Corps, Naval Medical Leader and Professional Development Command, 8955 Wood Road Bethesda, MD 20889, USA.

[c]UIC Barcelona – Universitat Internacional de Catalunya, Josep Trueta s/n, 08195 Sant Cugat del Valles (Barcelona), Spain.

[d]IBEC– Institute for Bioengineering of Catalonia, Baldiri Reixac 15-21, 08028 Barcelona, Spain

*Corresponding authors: NGF: fisc0456@umn.edu and CA: cjaparicio@uic.es

Declaration of interests

The authors declare that they have no known competing financial interests or personal relationships that could have appeared to influence the work reported in this paper.

Author contributions

All authors gave their final approval and agreed to be accountable for all aspects of the work.

John A. Pizarek: Methodology; Investigation; Visualization; Writing - Original Draft; Writing - Review & Editing; Data curation

Nicholas G. Fischer: Conceptualization; Methodology; Investigation; Visualization; Formal analysis; Supervision; Writing - Review & Editing; Data curation

Conrado Aparicio: Conceptualization; Methodology; Validation; Formal analysis; Resources; Funding acquisition; Supervision; Writing - Review & Editing

Acknowledgments

The authors thank Prof. Kim Mansky and Prof. Sven-Ulrik Gorr for equipment access, Mrs. Kristina Astleford-Hopper and Mr. Ravi Maisuria for their expertise and technical assistance with cell experiments. This work was supported by the NIH/NIDCR under awards R01DE026117 (CA), F30DE029105 (NGF), and T90DE0227232 (NGF). The content is solely the responsibility of the authors and does not necessarily represent the official views of the National Institutes of Health. The work was also supported by a 3M Science and Technology Fellowship (NGF). Parts of this work were carried out in the University of Minnesota I.T. Characterization Facility, which receives partial support from NSF through the MRSEC program. Figures were partially created with BioRender. JAP is a military Service member. This work was prepared as part of his official duties. Title 17, U.S.C., §105 provides that copyright protection under this title is not available for any work of the U.S. Government. Title 17, U.S.C., §101 defines a U.S. Government work as a work prepared by a military Service member or employee of the U.S. Government as part of that person's official duties. Opinions, interpretations, conclusions, and recommendations are those of the authors and are not necessarily endorsed by the Department of the Navy, Department of Defense, nor the U.S. Government.

Immunomodulatory IL-23 receptor antagonist peptide nanocoatings for implant soft tissue healing

Abstract

Objective: Peri-implantitis, caused by an inflammatory response to pathogens, is the leading cause of dental implant failure. Poor soft tissue healing surrounding implants – caused by inadequate surface properties – leads to infection, inflammation, and dysregulated keratinocyte and macrophage function. One activated inflammatory response, active around peri-implantitis compared to healthy sites, is the IL-23/IL-17A cytokine axis. Implant surfaces can be synthesized with peptide nanocoatings to present immunomodulatory motifs to target peri-implant keratinocytes to control macrophage polarization and regulate inflammatory axises toward enhancing soft tissue healing.

Methods: We synthesized an IL-23 receptor (IL-23R) noncompetitive antagonist peptide nanocoating using silanization and evaluated keratinocyte secretome changes and macrophage polarization (M1-like "pro-inflammatory" vs. M2-like "pro-regenerative").

Results: IL-23R antagonist peptide nanocoatings were successfully synthesized on titanium, to model dental implant surfaces, and compared to nonfunctional nanocoatings and non-coated titanium. IL-23R antagonist nanocoatings significantly decreased keratinocyte IL-23, and downstream IL-17A, expression compared to controls. This peptide noncompetitive antagonistic function was demonstrated under lipopolysaccharide stimulation. Large scale changes in keratinocyte secretome content, toward a pro-regenerative milieu, were observed from keratinocytes cultured on the IL-23R antagonist nanocoatings compared to controls. Conditioned medium collected from keratinocytes cultured on the IL-23R antagonist nanocoatings polarized macrophages toward a M2-like phenotype, based on increased CD163 and CD206 expression and reduced iNOS expression, compared to controls.

Significance: Our results support development of IL-23R noncompetitive antagonist nanocoatings to reduce the pro-inflammatory IL-23/17A pathway and augment macrophage polarization toward a pro-regenerative phenotype. Immunomodulatory implant surface engineering may promote soft tissue healing and thereby reduce rates of peri-implantitis.

Keywords: Surface chemistry; Keratinocyte; Macrophage; Peri-implant infection; Dental implant; Peptide

1.0 Introduction

The number of dental implants placed each year continues to increase; for instance, the percentage of United States adults with at least one tooth replaced with a dental implant is expected to be at least 17% by 2026 [1]. However, the prevalence of peri-implantitis is high and has been reported to range from 8% to 34% [2]. Peri-implant soft tissue attachment is composed of junctional epithelium, a keratinocyte-rich epithelial component with a basement membrane, enabling attachment to the implant surface through cell-matrix adhesive hemidesmosomes [3]. This junctional epithelium generated around dental implants is easier to penetrate than natural junctional epithelium around teeth due to reduced hemidesmosome formation, and thus less resilient to inflammatory challenges provoked by biofilms [4]. Chronic inflammation from peri-implant mucositis, augmented by parafunctional soft tissue attachment to the implant, leads to peri-implantitis. Bioengineered dental implant/abutment materials and surfaces for preventing peri-implantitis are therefore desirable.

Current surface modification approaches to prevent peri-implantitis have – largely – focused on using antimicrobials [5]. However, alternative implant surface modification technologies are necessary to "break the wave" of peri-implantitis [6]. Firstly, no Food and Drug Administration (FDA, USA) approved antimicrobial implant materials exist. Regulatory challenges include a lack of standardized antimicrobial testing protocols to match FDA guidance [7]. Secondly, peri-implantitis, should it develop, is typically managed by implantoplasty of the supracrestal area, implant surface detoxification, and hard tissue grafting of the intraosseous compartment [8]. However, there is no universally accepted protocol [6], surface detoxification harms implant surface characteristics [9], and only approximately 75% of implants survive following peri-implantitis treatments at 5 years [10]. Finally, the use of antimicrobial and antibiotic agents is under scrutiny given the "major threat" of antimicrobial resistance; 2019 saw an estimated 4.95 million deaths associated with antimicrobial resistance, a number that is expected to sharply rise in coming years [11].

Control over immunological responses that guide peri-implant soft tissue healing, with and without bacterial insult, is a potential strategy to help prevent peri-implant infection. Imbalances in pro-inflammatory activity have been reported as a greater concern for implant marginal bone loss than the dysbiotic biofilm in and of itself [12,13]. Certain cytokines mark inflammation in peri-implant soft tissue. IL-23, secreted by keratinocytes and other immune cells, is significantly upregulated in peri-implant crevicular fluid from peri-implantitis sites compared to healthy sites in clinical trials [14]. IL-23 has been implicated in other chronic inflammatory conditions, such as intestinal Crohn's disease, and closely associated with the influx of neutrophils in acute infections [15]. This, in turn, induces expression of pro-inflammatory factors like IL-17A, sustaining neutrophil recruitment and long-term maintenance of inflammation at the site of chronic bacterial infection [16]. IL-23 upregulates IL-17A expression through signal transducer and activator of transcription 3 (STAT3)-retinoid related orphan receptor-γ T (RORγT) [17]. IL-17 has been causally linked to periodontal bone loss [18].

Macrophages, derived from monocytes, are critically important to the initial soft tissue immune response and drive the conclusion of inflammation toward recruitment of reparative phase cell-types [19]. M1-like macrophages are prototypically "pro-inflammatory" where M2-like macrophages are prototypically "anti-inflammatory" and "pro-regenerative," although a continuum of macrophage phenotypes exist [20]. Macrophages are markedly polarized toward M1-like in peri-implantitis and periodontitis sites whereas M2-like macrophages pervade healthy gingival tissue [21]. Augmentation of macrophage phenotypes during inflammation has proven effective for disease treatment, such as cancer [22], and immune system responses to biomaterial implantation [23]. Dental implants and abutments engineered to polarize macrophages toward M2-like may be able to support prevention of peri-implantitis.

A recent and rapidly growing body of literature has begun to unravel the relationship between implant surfaces and macrophage polarization toward M1-like vs. M2-like [24]. For example, ample work

has demonstrated surfaces that polarize macrophages toward M2-like are beneficial for osseointegration [25]. Our group has established titanium coating silanization synthesis methods to form nanometric thickness peptide coatings [26–28]. Peptide nanocoatings harness biological activity of large, difficult-to-manufacture biomacromolecules in a small molecule and provide high bioactive specificity, versatility over orientation and multicomponent display of functions, and potential spatial/temporospatial control of bioactivity at the implant/wound site interface [29]. Potential drawbacks include the relatively small dosage of the peptide bioactive agent and limited half-life of peptides at room temperature [30]. One candidate peptide molecule capable of altering the immune system, commonly used in the pharmaceutical industry, are noncompetitive antagonists that bind to an allosteric site on a receptor to prevent receptor activation. Prior research identified an eight amino acid peptide that specifically bound to IL-23R as a noncompetitive antagonist and inhibited downstream IL-23 expression and signaling in spleen cells [31].

Thus, we aimed to immobilize a peptide noncompetitive antagonist on titanium against a pro-inflammatory signal – IL-23 – to ultimately polarize macrophages toward M2-like as opposed to M1-like.

Our hypothesis was that IL-23R antagonist peptide nanocoatings would decrease keratinocyte IL-23 and IL-17A expression, shift the keratinocyte secretome toward a pro-regenerative state, and polarize macrophages toward M2-like activity compared to nonfunctional, randomized sequence control peptide nanocoating and non-coated gold-standard control titanium surface (summarized in Supplemental Figure 1).

2.0 Materials and Methods

All materials were used as received. Sample sizes are denoted for each experimental technique.

2.1 Peptides nanocoating synthesis and characterization

An all-D amino acid IL-23 receptor antagonist (also known as peptide 2305, ylqqeeet), and a randomized sequence of the same amino acids generated with a random letter sequencer used as a control (tqyleeqe), were used in this study [31]. Lower case letters indicate D-amino acids whereas upper case letters indicate L-amino acids. A randomized peptide control was used to isolate potential effects from the non-specific physicochemistry created by the IL-23R peptide antagonist in comparison to the bioactive peptide structure dependent on the specific order of amino acids in the IL-23R antagonist sequence. The N-terminal tail of each peptide was modified with two lysines for preferential titanium surface immobilization on the N-terminus and three glycine spacers to allow flexibility of the tethered peptide [32,33]. The final functional peptide sequence (KK-GGG-ylqqeeet) and its randomized, control counterpart (KK-GGG-tqyleeqe) were synthesized using standard solid-phase peptide synthesis (>95% purity; AAPPTec) and characterized by high-performance liquid chromatography (HPLC) and electrospray (ESI) mass spectrometry (Supplemental Figures 2 and 3).

Nanocoatings were formed following our previous methods [26,27]. Titanium (commercially pure titanium grade II, McMaster Carr) disks were punched, ground, polished, and were treated with 5M NaOH for 12 hours to obtain activated titanium (**Non-coated**). Activated disks were placed in an N_2-rich atmosphere and immersed in pentane containing 0.05M N,N-Diisopropylethylamine and 0.5M (3-Chloropropyl)-triethoxysilane (all obtained from Sigma-Aldrich) to silanize the surface. These silanized disks were then immersed in 0.1 mM peptide solutions (IL-23 receptor antagonist or randomized control) in 0.1 M Na_2CO_3 buffer overnight to yield the **IL-23R Antagonist** and the **Randomized** control peptide nanocoatings, respectively.

Surface synthesis was characterized by an X-ray photoelectron spectrometer (XPS; PHI 5000 VersaProbe III, ULVAC Inc.) to quantify the surface elemental composition with a monochromatic Al Kα X-ray source (45°, 1486.6 eV, 50 W, sampling area; 200-µm diameter). Survey spectra were collected using a pass energy of 280 eV and a step size of 1.0 eV. Charge compensation was used, and spectra

were calibrated to the C 1s signal at 284.8 eV. Surface elemental composition [as atomic composition (At %)] was determined using MultiPak (ULVAC Inc.) from background-subtracted (system optimized) peak areas (n>3).

Water contact angle were measured using the sessile-drop method (>18 MΩ deionized water; 2.0 µL) to assess wettability of the surfaces using a contact angle goniometer (DM-CE1, Kyowa) and fit using the circle method (n=3 for Non-coated and n=10 for Il-23R Antagonist Nanocoatings and Randomized). Fewer samples were used for the Non-coated group given we have previously established the wettability properties of this surface [26,27].

The peptide nanocoatings were visualized with cyanine5 (43020, Lumiprobe) labeled peptides and an upright fluorescence microscope (DM 6B, Leica; 0.32 PH1 at 1296 × 966 pixels) (n>2). The fluorescent cyanine-5 N-hydroxysuccinimide (NHS) ester was dissolved in a 1/10 reaction volume of dimethylformamide (DMF) and added to the titanium disks that were immersed in 9/10 reaction volume of 0.1M sodium bicarbonate buffer (pH = 8.3) and allowed to react at 4 °C overnight. In total, 1 mg of cyanine-5 NHS ester was dissolved in 500 mL solution. The fluorescent cyanine-5 NHS ester was desorbed from disks in fresh sodium bicarbonate buffer for 5 minutes, with sonication, 7 times before disks were analyzed in Fiji [34]. Completely untreated, as received disks, were used to set a background threshold before micrographs were exported from Fiji to visually inspect the nanocoating homogeneity.

Peptide surface density was measured by comparing peptide solution concentration before and after disk immersion with a NanoOrange protein quantification kit (N6666, Thermo-Fisher) and a standard curve following the manufacturer's instructions to determine the peptide surface density ($\mu M/cm^2$) per disk (n=3) [35]. A plate reader (Synergy HT, Biotek) was used. Our previous work has established peptide coatings using an exceptionally similar synthesis method are a few nm thick [28].

2.2 Oral keratinocyte culture and proliferation

All materials, prior to all cell culture, were treated for 15 minutes per side with UV light in a biological safety cabinet (AC2-4S9-NS, Esco Lifesciences), adsorbed with bovine serum albumin (BSA) for 30 minutes, and finally washed with phosphate buffer solution (PBS). Immortalized human OKF6/TERT-2 (BWH Cell Culture and Microscopy Core, Boston, MA, USA) oral keratinocytes from normal tissue from the floor of the mouth were cultured in defined keratinocyte serum-free medium (Gibco) with 1% penicillin/streptomycin antibiotics (Gibco) under standard conditions [36]. For cell metabolic activity analysis, keratinocytes were seeded (6×10^4), cultured for either 1, 3, or 5 days, and then washed in PBS and incubated for four hours in CCK8 solution (Dojindo; 9:1 CCK8: keratinocyte medium). Optical density (OD) was obtained on a plate reader. OD values were blanked with virgin CCK8 solution and similarly incubated (n=5). Keratinocyte morphology was visualized with DAPI (4',6-diamidino-2-phenylindole dihydrochloride; D1306, Sigma-Aldrich) and conjugated phalloidin (R415, Thermo-Fisher) staining. All experiments, except keratinocyte secretome production, were performed with one sample in one well of a 48 well culture plate.

2.3 Keratinocyte IL-23 and IL-17A production

Keratinocyte expression of IL-23 and IL-17A was measured using enzyme-linked immunoassays (ELISAs). Keratinocytes were seeded on disks (1×10^4 cells per disk) and cultured for 6, 12 and 24 hours (n=3). Conditioned medium was collected, and disks were moved to a new plate for lysis (with protease inhibitor, 78429, Thermo Scientific). Lysate was cleared (12,000 *g* for ten minutes) and then combined 1:1 (by volume) with conditioned medium. IL-23 (ab221837, Abcam) and IL-17A (ab216167, Abcam) production was measured by ELISA following the manufacturer's instructions.

In some experiments, a pro-inflammatory stimulus, ultrapure *Porphyromonas gingivalis* lipopolysaccharide (LPS; tlrl-ppglps, InvivoGen), was used to provide an induction of inflammatory response at 0.1µg/mL [37] for 24 hours. LAL (limulus amebocyte lysate) treated endotoxin free water

was used as a vehicle control for LPS experiments. Total protein was determined with a micro bicinchoninic acid assay (23235, Thermo Fisher) as described by the manufacturer for normalization.

2.4 Keratinocyte cytokine and chemokine production

Keratinocyte secretome production was measured by culturing keratinocytes (1×10^4 per disk) for one day. Six disks were pooled per analysis in a 6 well culture plate. Conditioned medium was collected, and disks were moved to a new plate for lysis (with protease inhibitor, 78429, Thermo Scientific). Lysis was performed to collect all chemokines and cytokines produced by the keratinocytes, including those not yet secreted. Lysate was cleared (12,000 *g* for ten minutes) and then combined 1:1 (by volume) with conditioned medium. Cytokine production was measured with a cytokine array (AAH-TH17-1-2, RayBiotech) following the manufacturer's instructions; each cytokine was probed in technical duplicate. This array was used to probe a wider range of cytokines and chemokines in a single experiment compared to ELISAs. The cytokines measured include, CCL20, CD40, CD40LG, CSF2, CSF3, IFNG, IFNL2, IL10, IL12A, IL12B, IL13, IL17A, IL17F, IL17RA, IL1B, IL1R1, IL1R2, IL2, IL21, IL21R, IL22, IL23A, IL4, IL5, IL6, IL6R, IL6ST, LTA, TGFB1, TGFB3, TNF, TNFRSF18, TNFRSF8, TNFSF11. ImageJ was used to analyze and collect the background, positive control, negative controls, and the array data. Background subtraction was completed for each array datapoint, with the average of two background samples per datapoint, along with positive control normalization between all data points.

STRING analysis, or Search Tool for the Retrieval of INteracting Genes/proteins, a database and online resource for known and predicted protein-protein interactions, was used. All 34 proteins, and associated concentration measured, from the assay were input into the system to see how they interact. The lines connecting nodes have different colors based on how the interaction was determined, such as from databases or experimentally determined [38].

2.5 Macrophage culture and polarization

Primary human peripheral blood mononuclear cells (PBMCs) were obtained as a Trima Cone from Innovate Blood Resources (deidentified, for research use only) and cultured in ImmunoCult-SF macrophage medium (10961, STEMCELL Technologies; contains macrophage colony-stimulating factor) on tissue culture plastic to obtain plastic-adherent monocytes [39]. Cells were cultured for 4 days and then activated toward either M1-like (10 ng/mL LPS and 50 ng/mL interferon gamma; 78020 STEMCELL Technologies), M2-like (10 ng/mL interleukin-4; 78045, STEMCELL Technologies) or in 2:1 or 1:1 dilutions of macrophage medium with keratinocyte-conditioned medium for 2 day (Supplemental Figure 4). Despite limited work on keratinocyte-conditioned medium for macrophage culture, we followed a previous report for myofibroblasts and macrophages using a 1:1 medium ratio [40]. The additional 2:1 dilution was used to evaluate potential concentration-specific effects. Controls with non-conditioned keratinocyte medium were also performed (Supplemental Figure 5). Keratinocyte-conditioned medium was collected as described for cytokine analysis then combined with macrophage medium as described.

After activation for 2 days in described mediums, macrophages were fixed in 4% paraformaldehyde for 20 minutes, permeabilized in 0.3% Triton X-100 for 5 minutes, and blocked in SuperBlock (37515, Thermo Fisher) for 20 minutes. Samples were washed in PBS thrice between all steps. Macrophage polarization was evaluated with surface marker analysis using CD68 as a pan-macrophage marker, iNOS as a M1-like marker, and CD206 and CD163 as M2-like markers (all at 1:200 at 4°C overnight; ARG30333, argio Biolaboratories). Secondary antibodies (ab97037, Abcam and A-11034, Invitrogen) were diluted (1:400) and applied at 4°C overnight. Immunofluorescent visualization was performed with an upright fluorescent microscope (DM 6B, Leica). Background-subtracted pixel intensities were calculated and analyzed in Fiji using the area integrated density function. All values were normalized to the total number of cells per field of view, which was manually calculated. Four wells, with three micrographs each, were taken per group.

2.6 Statistics

All biological experiments described were independently repeated twice (in addition to the noted technical replicates). Specific statistical tests and interpretations used for each experiment are described in captions for each figure. Statistical significance was denoted by use of letters; groups not sharing a letter are statistically significantly different from others ($\alpha = 0.05$). Letters, as opposed to asterisks, were used for thorough visualization of statistical analysis results given some graphs display 35 pairwise comparisons. GraphPad Prism 9.3.1 (GraphPad Software) was utilized to perform all statistical analysis, with one exception as multivariate analysis (Ward's clustering) was performed for Figure 3 in JMP Pro 14 (JMP Statistical Discovery LLC).

3.0 Results

3.1 IL-23R antagonist peptide Nanocoatings and controls were successfully synthesized

The physicochemical properties of model titanium dental implant surfaces with IL-23R Antagonist and the Randomized peptide Nanocoatings were compared to control titanium (Non-coated). There were no significant differences between water contact angles for all tested surfaces (ca. 15°; Figure 1a and 1b), which was expected given the ratio of hydrophilic residues to total number of residues for the peptides is 63%. Nanocoatings made of fluorescently labeled peptides revealed an intense fluorescence signal, evenly distributed, on both Randomized and IL-23R Antagonist, unlike Non-coated surfaces (Figure 1c).

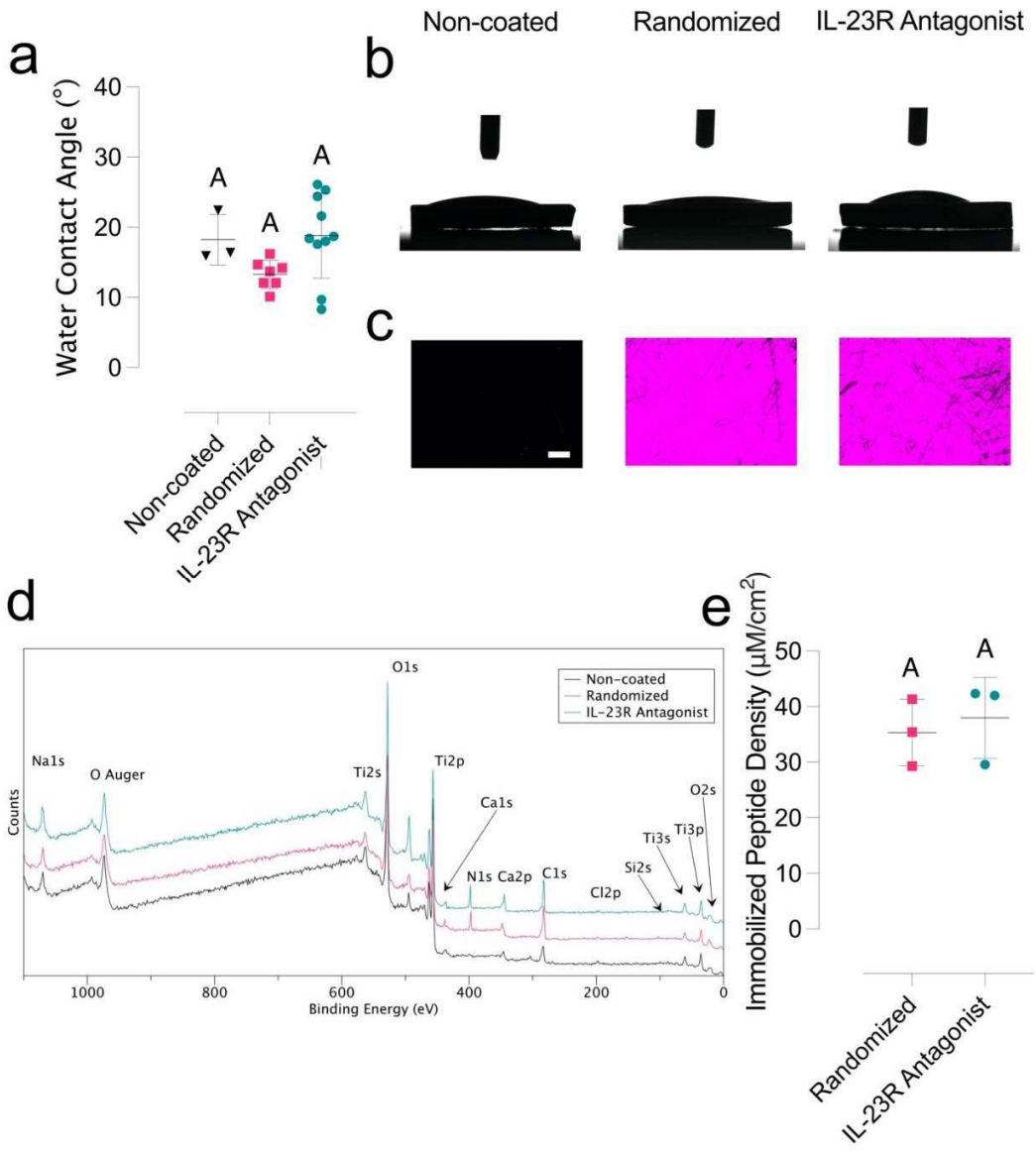

Figure 1: Homogeneous IL-23R antagonist and randomized peptides Nanocoatings were synthesized on titanium surfaces. a: Water contact angles of Non-coated, Randomized, and IL-23R Antagonist Nanocoatings. Dissimilar letters indicate statistically significant differences (one-way ANOVA; $p < 0.05$) when all groups are compared to each other. **b:** Representative micrographs of water contact angles formed on Non-coated, Randomized, and IL-23R Antagonist Nanocoatings. **c:** Fluorescent visualization of fluorescently labeled Non-coated, Randomized, and IL-23R Antagonist Nanocoatings. Scale bars are 100 µm for the lower panel. **d:** X-ray photoelectron survey spectra of Non-coated, Randomized, and IL-23R Antagonist Nanocoatings. Peaks for elements of interest are marked. **e:** Immobilized peptide surface density of Randomized and IL-23R Antagonist Nanocoatings assessed using NanoOrange©. Dissimilar letters indicate statistically significant differences (one-way ANOVA; $p < 0.05$) between all groups. However, Figure 1e was compared with a *t*-test; ($p > 0.05$) instead. All scatter dot plots also show mean ± standard deviation for each group.

Moreover, XPS detected (Figure 1d and Supplemental Table 1) a notable peptide-signature N1s peak, for both Antagonist (10.04 ± 0.73 At%) and Randomized (11.54 ± 0.73 At%) compared to Non-coated (0.04 ± 0.73 At%) surfaces. Finally, the surface peptide density was quantified using a NanoOrange© assay. No significant differences were observed between IL-23R Antagonist and Randomized peptide Nanocoatings (Figure 1e). These data overall demonstrated successful synthesis of IL-23R Antagonist and Randomized Nanocoatings with no significant differences in physical-chemical properties and surface peptide densities.

3.2 IL-23R Antagonist Nanocoatings reduce IL-23 and downstream IL-17A production compared to controls

Keratinocytes were initially cultured for up to five days to evaluate the IL-23R Antagonist Nanocoating cytocompatibility. No differences in keratinocyte morphology (Supplemental Figure 6) nor metabolic activity (Supplemental Figure 7) were seen between Randomized, Antagonist, and Non-coated, a gold-standard cytocompatible surface. To test our hypothesis that IL-23R Antagonist Nanocoatings reduce keratinocyte IL-23 and IL-17A expression compared to controls, we collected conditioned medium and quantified cytokines at 6, 12 and 24 hours after keratinocyte seeding using enzyme-linked immunoassays (ELISAs). All cell culture experiments were performed on surfaces pre-sorbed with bovine serum albumin to reduce nonspecific interactions. IL-23 expression (Figure 2a; specific p-values are in Supplemental Table 2) from keratinocytes cultured on the IL-23R Antagonist Nanocoatings was significantly lower than on Randomized Nanocoatings and Non-coated surfaces. No differences in IL-23 expression were assessed between Non-coated and Randomized, suggesting that surface physicochemistry played little biological significance compared to the presence of peptide sequence and

structure of the IL-23R Nanocoatings. IL-17A expression was similarly reduced at the terminal 24 hour time point on IL-23R Antagonist compared to Randomized and Non-coated (Figure 2b).

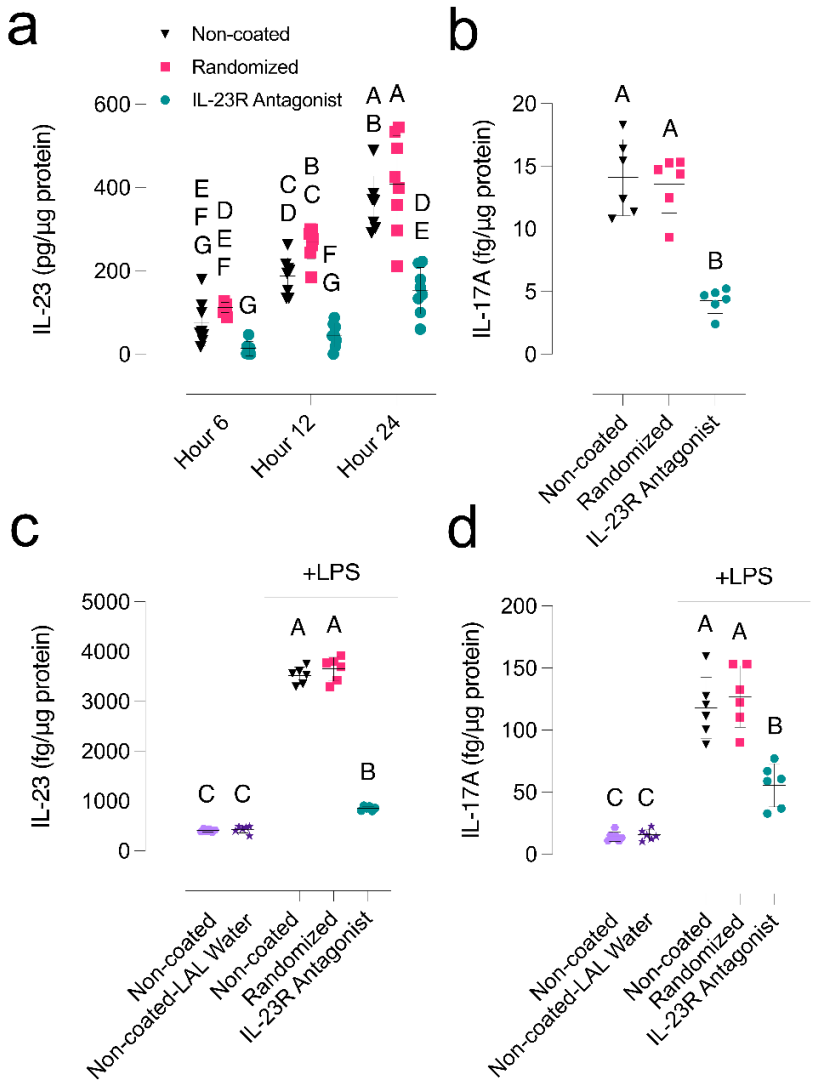

Figure 2: The IL-23R Antagonist Nanocoating significantly decreased production of IL-23 and IL-17A, both without and with LPS stimulus. a: Unstimulated keratinocyte IL-23 expression on Non-coated, Randomized, and IL-23R Antagonist Nanocoatings after 6, 12, and 24-hour culture. Dissimilar letters indicate statistically significant differences (two-way ANOVA; $p < 0.05$) when all groups are compared to each other. **b:** Unstimulated keratinocyte IL-17A expression on Non-coated, Randomized, and IL-23R Antagonist Nanocoatings after 24-hour culture. Dissimilar letters indicate statistically significant differences (two-way ANOVA; $p < 0.05$) when all groups are compared to each other. **c** and **d:** IL-23 (**c**) and IL-17A (**d**) expression from LPS-stimulated (+LPS) keratinocytes Non-coated, Randomized, and IL-23R Antagonist Nanocoatings after 24-hour culture. Non-coated-LAL water was tested as an LPS vehicle

control. Dissimilar letters indicate statistically significant differences (two-way ANOVA; $p < 0.05$) when all groups are compared to each other. All scatter dot plots also show mean ± standard deviation for each group.

We then investigated the ability of our nanocoatings to remain potent under an inflammatory stimuli of 0.1 μg/mL *P. gingivalis* LPS stimulus compared to unstimulated Non-coated and LPS vehicle (LAL water) controls at 24 hours. Again, keratinocyte IL-23 (Figure 2c) and IL-17A expression (Figure 2d), under this more oral simulative culturing condition, was reduced on the IL-23R Antagonist Nanocoatings compared to Randomized and Non-coated. These data validated our hypothesis that IL-23R Nanocoatings are both cytocompatible and biologically active to reduce keratinocyte IL-23 and IL-17A expression.

3.3 IL-23R Antagonist Nanocoatings decrease keratinocyte pro-inflammatory cytokine expression compared to controls

We next hypothesized larger scale secretome changes – compared to just IL-23 and IL-17A – were occurring from the noncompetitive antagonist action of the IL-23R Antagonist Nanocoatings. We profiled periodontally-relevant cytokine and chemokine expression by keratinocytes cultured on IL-23R Antagonist, Randomized, and Non-coated surfaces (Figure 3a). The normalized, relative to Non-coated, expression is specified by the red (increase) to green (decrease) color. IL-23R Antagonist Nanocoatings reduced IL-17A, IL-17F, IL-23, glycoprotein 130 (gp130), and IL-6 expression, while macrophage inducing peptide (MIP)-3a, IL-2, IL-1R1 and interferon gamma (IFN-γ) production were increased, in comparison to Non-coated. Randomized showed a decrease in MIP-3a, IFN-γ, IL-2, IL-1R1, and IL-23 and an increase in IL-6, gp130, IL-5, IL-21R, tissue growth factor beta-1 (TGFβ1), and IL-13, in comparison to Non-coated. STRING (Search Tool for the Retrieval of INteracting Genes/proteins) analysis revealed all evaluated chemokines and cytokines were known interactors with key cytokine IL-17A (note its relative central

location) on IL-23R Antagonist Nanocoatings (Figure 3b). Indeed, as suggested by the many cytokine and chemokine expression changes seen, strong interactions were found between the majority of cytokines and chemokines. In sum, these results validated our hypothesis that IL-23R Nanocoatings could increase keratinocyte pro-reparative/anti-inflammatory expression of many cytokines and chemokines compared to controls through IL-17A.

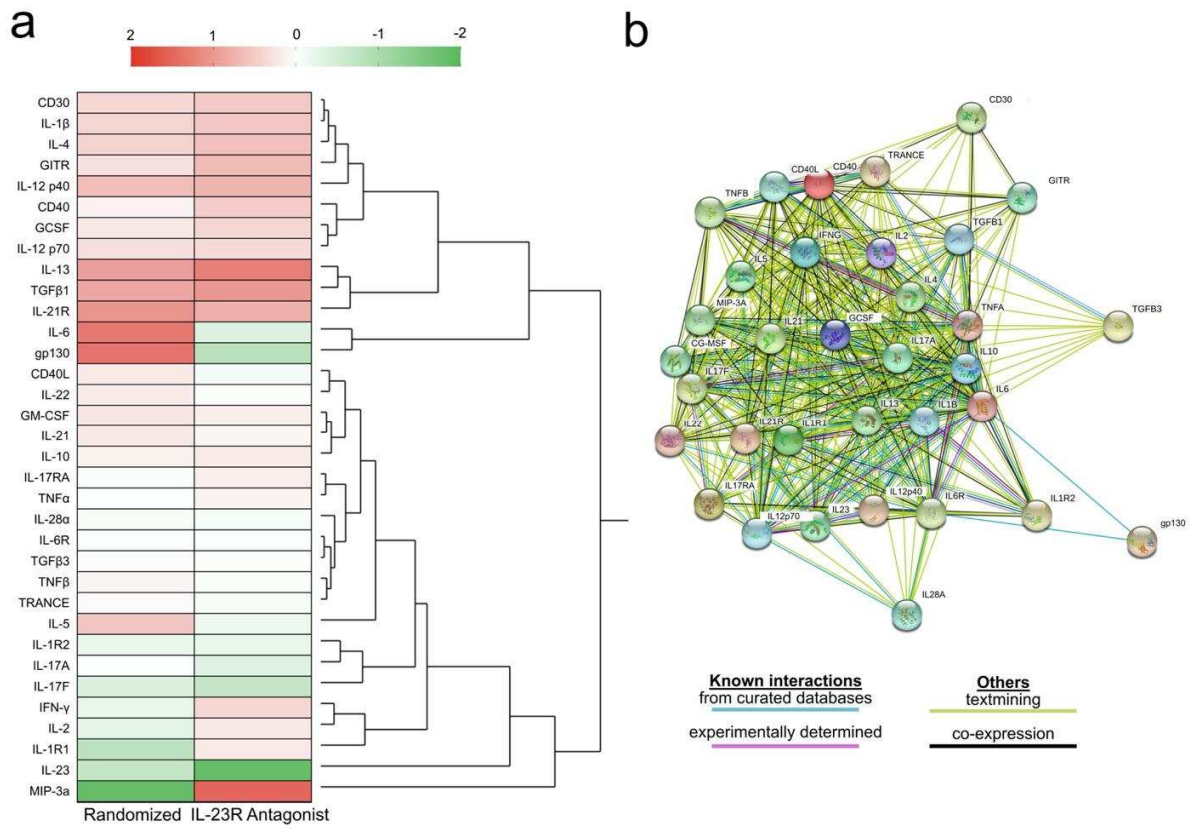

Figure 3: **IL-23R Antagonist Nanocoating lead to broad downstream effects, decreasing the pro-inflammatory signals of keratinocytes through control of just IL-23R. a:** Cytokine/chemokine secretome by keratinocytes on Randomized and IL-23R Antagonist Nanocoatings compared to Non-coated (expression, as a mean, is shown as transformed sine(x)log(1 + |x|). Ward's clustering was used to create the dendrogram to group cytokines/chemokines by the similarity between them. **b:** STRING (Search Tool for the Retrieval of INteracting Genes/proteins) analysis of the interaction of all cytokines on keratinocytes IL-23R Antagonist Nanocoatings. Blue lines represent known interactions from curated

databases, and pink represents experimentally determined interactions. Light green lines represent interactions determined by text mining and black represents the co-expression of the two proteins [38].

3.4 IL-23R Antagonist Nanocoatings polarize macrophages toward a pro-regenerative M2-like phenotype compared to controls

Given the changes in secretome by keratinocytes on IL23R Antagonist Nanocoatings we finally hypothesized that these coatings regulate immune responses and polarize PBMCs toward a M2-like macrophage phenotype ("pro-regenerative;" CD163-high and CD206-high) compared to M1-like ["pro-inflammatory;" inducible nitric oxide synthase (iNOS)-high] (Figure 4a). Note we hypothesized M1-like and M2-like phenotypes, rather than M1 and M2, given macrophage phenotypes exist on a large spectrum, rather than discrete, binarized classes [41]. PBMCs were cultured and exposed to conditioned medium from keratinocytes grown on IL-23R Antagonist, Randomized, and Non-coated surfaces. Standard cytokine cocktails were used to differentiate PBMCs toward gold-standard M1-like and M2-like for comparison. Immunofluorescence analysis of iNOS (M1-like) demonstrated (Figure 4b and Supplemental Figure 8) the conditioned medium from IL-23R Antagonist Nanocoatings induced lower expression compared to Randomized and Non-coated. In tandem, CD163 and CD206 (M2-like) expression (Figure 4c and Supplemental Figure 8) was highest on PBMCs cultured on IL-23R Antagonist compared to Randomized and Non-coated conditioned media and was statistically insignificant from the positive M2-like control. These results soundly validated our hypothesis that, through keratinocyte activity, IL-23R Antagonist Nanocoatings could exert functionally significant effects on macrophage polarization toward providing a pro-regenerative phenotype to improve soft tissue healing around dental implants.

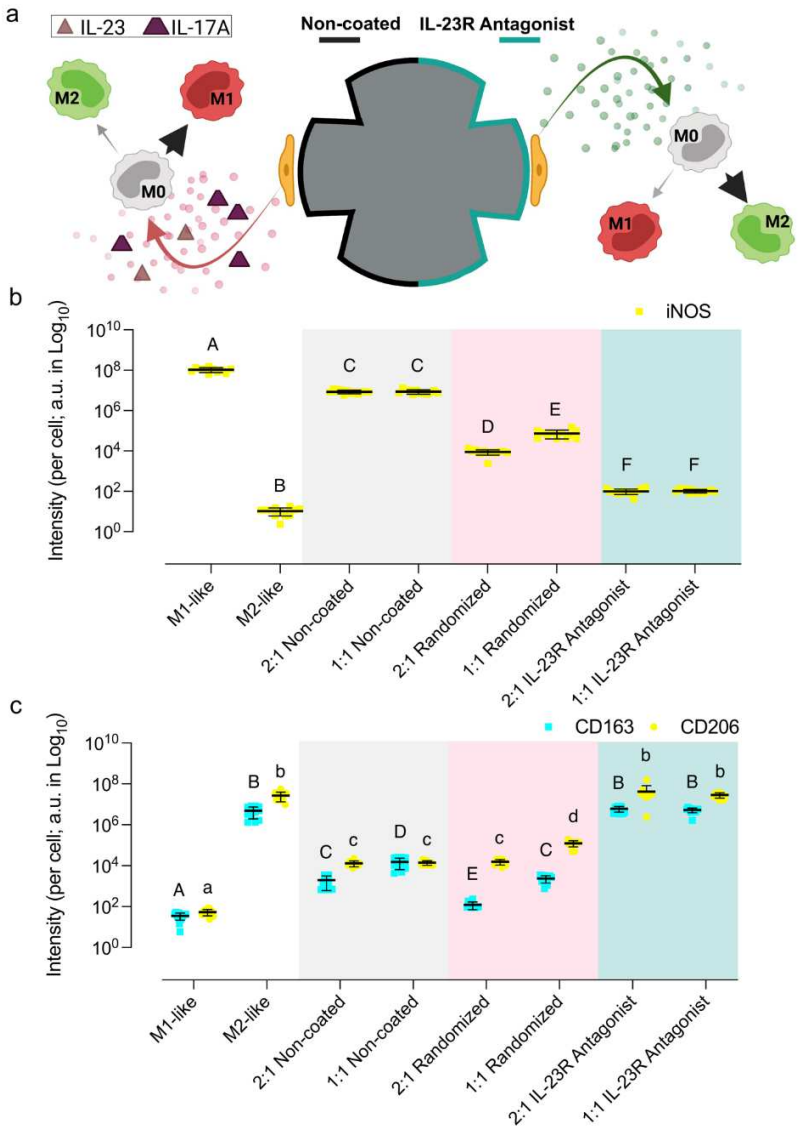

Figure 4: IL-23R Antagonist Nanocoatings causes differences in oral keratinocyte secretions leading to significantly altered signaling to macrophages, producing more M2-like macrophages a: Schematic summarizing increased expression of IL-23 and IL-17A expression on Non-coated compared to IL-23R Antagonist Nanocoatings leading to hypothesized increased M1-like macrophage phenotype (iNOS expression) vs. predominant M2-like macrophage phenotype (CD163 and CD206 expression) **b**: Immunofluorescent quantification of iNOs expression [log_{10} arbitrary units (a.u.)] of control M1-like and M2-like macrophages as well as PBMCs exposed to 2:1 and 1:1 ratios of keratinocyte-conditioned medium from Non-coated, Randomized, and IL-23R Antagonist Nanocoatings. Dissimilar letters indicate statistically significant differences (two-way ANOVA; $p < 0.05$) when all groups are compared to each other. **c.** Immunofluorescent quantification of macrophage CD163 and CD206 expression [log_{10} arbitrary units (a.u.)] of control M1-like and M2-like macrophages as well as PBMCs exposed to 2:1 and 1:1 ratios of keratinocyte-conditioned medium from Non-coated, Randomized, and IL-23R Antagonist Nanocoatings. Dissimilar letters indicate statistically significant differences (two-way ANOVA; $p < 0.05$)

when all groups are compared to each other. All scatter dot plots also show mean ± standard deviation for each group.

4.0 Discussion

The junction between soft tissues and the implant serves as the first biological defense mechanism against ingression of pathogens that initiates peri-implantitis [42]. No well-established treatment modalities exist for peri-implantitis. Here, as a preventative measure, we synthesized biocompatible nanocoatings composed of IL-23R noncompetitive antagonists to reduce keratinocyte IL-23 and downstream IL-17A expression under normal and conditioned LPS-stimulated culture. This can be of clinical relevance given IL-23 is significantly upregulated in peri-implant crevicular fluid from peri-implantitis sites compared to healthy sites [14] and IL-17 can drive periodontal bone loss [18]. We also found larger scale, pro-regenerative secretome changes. These changes skewed macrophage polarization toward a pro-regenerative M2-like phenotype compared to controls. Overall, our approach for optimizing peri-implant soft tissue healing moves past common antimicrobial technologies toward immunomodulatory implant materials that are expected to reduce peri-implantitis rates and the associated oral healthcare burden.

Recent work [43] compared the junctional epithelium associated with implants, also known as peri-implant epithelium, to natural junctional epithelium and found the implant-associated junctional epithelium lacked a stem cell niche, had reduced attachment, and was marked by a robust inflammatory cell infiltrate. Other functional differences have been summarized elsewhere [3,44]. Biomaterial researchers have responded by developing cell-adhesive surfaces [reviewed elsewhere [45]] to fortify these vulnerable interfaces. Approaches are typified by biomolecular or physicochemical surface modification [46]; initial examples of their translation into commercial abutments and implants may be found. However, oral mucosal immunity too plays a broad influence in factors critical to implant success.

For example, alveolar bone destruction from dysbiotic biofilms have been tied to T-cell population expansion, recruitment of neutrophils, and prolonged expression of type I interferons [47].

As a consequence, others have undertaken inspiring work to modulate the peri-implant immune system, such as developing implant surface-mediated delivery of IL-4 [48], locally delivered C-C motif chemokine ligand 2 (CCL2) [49], and anionic linoleic acid coatings [50]. These works recognize that while an intense focus in the literature on antimicrobial solutions to peri-implantitis has pervaded, more recent work supports the idea that bacterial antagonism of tissues is secondary to immune responses toward dictating implant survival/failure. For example, macrophages are markedly polarized toward M1-like in peri-implantitis and periodontitis whereas M2-like pervades healthy gingival tissue [21]. Our Nanocoatings here skewed macrophages toward an M2-like phenotype. We particularly note upregulation of MIP-3a and downregulation of IL-16 and gp130. MIP-3a has been associated with M2-like macrophage polarization and IL-16 and gp130 have been associated with M1-like macrophages [51,52]. Future work is needed to understand why MIP-3a expression differs so much between IL-23R Antagonist and Randomized. This may be important given MIP-3a is a potent chemokine for dendritic cells [53]. We also observed IL-23R Antagonist Nanocoatings reduced IL-16, which is increased in peri-implant mucositis compared to healthy implants [54], and IL-13 was upregulated on Randomized, which is correlated with peri-implantitis inflammation progression [55]. We finally noted Randomized showed the most notable differences between 1:1 and 2:1 conditioned medium ratios. We speculate these dosage differences were due to the stronger signaling arising from the conditioned medium compared to weaker non-specific physicochemical-mediated signaling from the Randomized surface.

A final interesting observation was that Randomized nanocoatings reduced iNOS expression compared to Non-coated surfaces, although not as much as IL-23R Antagonist Nanocoatings, suggesting, at least a partial role for peptide nanocoating physicochemistry (and not necessarily peptide structure) in altering macrophage phenotype. One limitation of our work is the focus on CD206, CD163, and iNOs

to evaluate macrophage phenotypes. Further work is needed to define macrophage elaborations that our nanocoatings induce, particularly as it relates to M1-like and M2-like function like CD197, CXCL10, and IL-10. Other further work is needed to relate cytokines classically related to the IL-23 pathway - IL-1β, IL-6, IFN-γ, and TNF-α [56] - to macrophage M1-like and M2-like function. Much of the literature's focus on IL-23 and IL-17A is in the content of T-helper cells [57]; but expanded understanding of the roles in macrophage function in the oral cavity is missing.

The present approach offers potential advantages. D-enantiomer amino acids were used based on the original in silico design of the IL-23R antagonist peptide [31]. D-enantiomer peptides, unlike commonly found L-enantiomers, are not associated with a robust immune response [58]. This "blank slate" of the nanocoating building block may potentially enable other immunomodulatory sequences to be designed with more finely-tuned effects than L-enantiomers. Indeed, we observed the IL-23R Antagonist Nanocoatings dramatically reduced IL-23 and IL-17A expression under LPS stimulation. This suggests strong interactions with the IL-23 receptor consistent with past work reporting the functional selectivity of the peptide sequence [31]. Functional selectivity achieved by the use of peptides is a highly appealing trait for immunomodulatory biomaterial surface design given the goal of modulating only a specific, "harmful" immune pathway and leaving other, "helpful" immune responses intact to promote biomaterial biocompatibility. A common disadvantage of therapeutic peptides and peptide-modified materials is their susceptibility to degradation. Indeed, only around 60 of 1,500 small molecules drugs approved by the FDA are peptides [59]. These are predominately L-enantiomers. One way to sidestep this challenge is D-enantiomers, which degrade markedly slower, and can thus potentially improve therapeutic potency. We and others have shown that peptide nanocoating synthesized with L-enantiomers are indeed resistant to insertion into polyurethane foam blocks simulating bone [60], storage in simulated saliva for seven weeks [61], and storage for six months [62]. Further work is necessary to firmly establish benefits of using D-enantiomer peptides compared to L-enantiomer.

Dental implant peptide nanocoatings harness the advantages of peptides and localize them for desired biological activity, such as antimicrobial activity or control of soft/hard tissue responses (Fischer et al. 2020b). For example, our group has used localized TGF-β1 inhibitor peptide nanocoatings toward reducing fibrosis during early implant osseointegration [28]. Indeed, vaccine delivery technologies have neatly shown that bolus delivery of therapeutics to provoke an immune response result in poor spatiotemporal responses compared to localized biomaterials-mediated delivery [63]. Peptide nanocoatings could be applied in dental implant manufacturing settings using relatively facile chemical processes and take advantage of large-scale peptide synthesis techniques used for peptide vaccines and therapeutics to reduce their otherwise high costs. Overall, peptides' polymeric nature and range of techniques for nanocoating synthesis offer a method for extreme control of implant surface chemistry.

Our future work will include evaluation in a pre-clinical animal model. We showed nanocoating antagonistic activity was retained under LPS stimulation but whether this holds true in an animal, with other pro-inflammatory stimuli and cells, needs to be verified. Indeed, while we clearly altered IL-17 and IL-23 signaling, the downstream effects on other cytokines and chemokines identified in Figure 3 may have unintended effects. Such experiments must be carefully designed as the Randomized nanocoating itself – likely through surface physical chemical alterations [64] – induced keratinocyte secretome changes. A broader remaining question is whether control of macrophage polarization is a clinically viable method to influence implant longevity. Certainly, macrophage activation dictates bone progenitor recruitment and inflammation resolution *in vivo* [65] but whether this will affect clinically relevant, long-term peri-implant soft tissue measures remains an open question.

5.0 Conclusion

We engineered and validated an IL-23R noncompetitive antagonist peptide nanocoating to reduce keratinocyte pro-inflammatory expression of IL-23 and IL-17A. Changes in the keratinocyte

secretome were able to skew macrophage polarization toward a pro-regenerative M2-like phenotype. These results inform immunomodulatory dental implant design and bioinspired surface biomolecular coatings to improve soft tissue attachment and healing resolution to thereby reduce the rate of peri-implantitis. These results may also drive innovation in other medical specialties with percutaneous devices, such orthopaedic osseointegrated limbs protheses, osseointegrated auditory devices, and catheters.

References

[1] H.W. Elani, J.R. Starr, J.D. Da Silva, G.O. Gallucci, Trends in Dental Implant Use in the U.S., 1999–2016, and Projections to 2026, J. Dent. Res. 97 (2018) 1424–1430. doi:10.1177/0022034518792567.

[2] K. Kordbacheh Changi, J. Finkelstein, P.N. Papapanou, Peri-implantitis prevalence, incidence rate, and risk factors: A study of electronic health records at a U.S. dental school, Clin. Oral Implants Res. 30 (2019) 306–314. doi:10.1111/clr.13416.

[3] N.G. Fischer, C. Aparicio, Junctional epithelium and hemidesmosomes: Tape and rivets for solving the “percutaneous device dilemma” in dental and other permanent implants, Bioact. Mater. 18 (2022) 178–198. doi:10.1016/j.bioactmat.2022.03.019.

[4] S. Ivanovski, R. Lee, Comparison of peri-implant and periodontal marginal soft tissues in health and disease, Periodontol. 2000. 76 (2018) 116–130. doi:10.1111/prd.12150.

[5] J.G.S. Souza, M.M. Bertolini, R.C. Costa, B.E. Nagay, A. Dongari-Bagtzoglou, V.A.R. Barão, Targeting implant-associated infections: titanium surface loaded with antimicrobial, IScience. 24 (2021) 102008. doi:10.1016/j.isci.2020.102008.

[6] J.H. Fu, H.L. Wang, Breaking the wave of peri-implantitis, Periodontol. 2000. 84 (2020) 145–160. doi:10.1111/prd.12335.

[7] F. Cieplik, C. Aparicio, J. Kreth, G. Schmalz, Development of standard protocols for biofilm-biomaterial interface testing, JADA Found. Sci. 1 (2022) 100008. doi:10.1016/j.jfscie.2022.100008.

[8] A. Monje, F. Schwarz, Principles of Combined Surgical Therapy for the Management of Peri-Implantitis, Clin. Adv. Periodontics. 12 (2022) 57–63. doi:10.1002/cap.10186.

[9] G.A. Kotsakis, C. Lan, J. Barbosa, K. Lill, R. Chen, J. Rudney, C. Aparicio, Antimicrobial agents used in the treatment of peri-implantitis alter the physicochemistry and cytocompatibility of titanium surfaces., J. Periodontol. (2016) 1–20. doi:10.1902/jop.2016.150684.

[10] L.J. Heitz-Mayfield, M. Aaboe, M. Araujo, J.B. Carrión, R. Cavalcanti, N. Cionca, D. Cochran, I. Darby, E. Funakoshi, P.C. Gierthmuehlen, D. Hashim, L. Jahangiri, Y. Kwon, F. Lambert, D.M. Layton, E.R. Lorenzana, G. McKenna, A. Mombelli, F. Müller, M. Roccuzzo, G.E. Salvi, M. Schimmel, M. Srinivasan, C. Tomasi, A. Yeo, Group 4 ITI Consensus Report: Risks and biologic

complications associated with implant dentistry, Clin. Oral Implants Res. 29 (2018) 351–358. doi:10.1111/clr.13307.

[11] C.J. Murray, K.S. Ikuta, F. Sharara, L. Swetschinski, G. Robles Aguilar, A. Gray, C. Han, C. Bisignano, P. Rao, E. Wool, S.C. Johnson, A.J. Browne, M.G. Chipeta, F. Fell, S. Hackett, G. Haines-Woodhouse, B.H. Kashef Hamadani, E.A.P. Kumaran, B. McManigal, R. Agarwal, S. Akech, S. Albertson, J. Amuasi, J. Andrews, A. Aravkin, E. Ashley, F. Bailey, S. Baker, B. Basnyat, A. Bekker, R. Bender, A. Bethou, J. Bielicki, S. Boonkasidecha, J. Bukosia, C. Carvalheiro, C. Castañeda-Orjuela, V. Chansamouth, S. Chaurasia, S. Chiurchiù, F. Chowdhury, A.J. Cook, B. Cooper, T.R. Cressey, E. Criollo-Mora, M. Cunningham, S. Darboe, N.P.J. Day, M. De Luca, K. Dokova, A. Dramowski, S.J. Dunachie, T. Eckmanns, D. Eibach, A. Emami, N. Feasey, N. Fisher-Pearson, K. Forrest, D. Garrett, P. Gastmeier, A.Z. Giref, R.C. Greer, V. Gupta, S. Haller, A. Haselbeck, S.I. Hay, M. Holm, S. Hopkins, K.C. Iregbu, J. Jacobs, D. Jarovsky, F. Javanmardi, M. Khorana, N. Kissoon, E. Kobeissi, T. Kostyanev, F. Krapp, R. Krumkamp, A. Kumar, H.H. Kyu, C. Lim, D. Limmathurotsakul, M.J. Loftus, M. Lunn, J. Ma, N. Mturi, T. Munera-Huertas, P. Musicha, M.M. Mussi-Pinhata, T. Nakamura, R. Nanavati, S. Nangia, P. Newton, C. Ngoun, A. Novotney, D. Nwakanma, C.W. Obiero, A. Olivas-Martinez, P. Olliaro, E. Ooko, E. Ortiz-Brizuela, A.Y. Peleg, C. Perrone, N. Plakkal, A. Ponce-de-Leon, M. Raad, T. Ramdin, A. Riddell, T. Roberts, J.V. Robotham, A. Roca, K.E. Rudd, N. Russell, J. Schnall, J.A.G. Scott, M. Shivamallappa, J. Sifuentes-Osornio, N. Steenkeste, A.J. Stewardson, T. Stoeva, N. Tasak, A. Thaiprakong, G. Thwaites, C. Turner, P. Turner, H.R. van Doorn, S. Velaphi, A. Vongpradith, H. Vu, T. Walsh, S. Waner, T. Wangrangsimakul, T. Wozniak, P. Zheng, B. Sartorius, A.D. Lopez, A. Stergachis, C. Moore, C. Dolecek, M. Naghavi, Global burden of bacterial antimicrobial resistance in 2019: a systematic analysis, Lancet. 399 (2022) 629–655. doi:10.1016/S0140-6736(21)02724-0.

[12] T. Albrektsson, C. Dahlin, D. Reinedahl, P. Tengvall, R. Trindade, A. Wennerberg, An Imbalance of the Immune System Instead of a Disease Behind Marginal Bone Loss Around Oral Implants: Position Paper, Int. J. Oral Maxillofac. Implants. 35 (2020) 495–502. doi:10.11607/jomi.8218.

[13] S. Amin Yavari, S.M. Castenmiller, J.A.G. Strijp, M. Croes, Combating Implant Infections: Shifting Focus from Bacteria to Host, Adv. Mater. 32 (2020) 2002962. doi:10.1002/adma.202002962.

[14] Z. Luo, H. Wang, Z. Sun, W. Luo, Y. Wu, Expression of IL-22, IL-22R and IL-23 in the peri-implant soft tissues of patients with peri-implantitis, Arch. Oral Biol. 58 (2013) 523–529. doi:10.1016/j.archoralbio.2012.08.006.

[15] G.P. Mardegan, J.A. Shibli, L.A. Roth, M. Faveri, G. Giro, M.F. Bastos, Transforming growth factor-β, interleukin-17, and IL-23 gene expression profiles associated with human peri-implantitis, Clin. Oral Implants Res. 28 (2017) e10–e15. doi:10.1111/clr.12846.

[16] B.S. McKenzie, R.A. Kastelein, D.J. Cua, Understanding the IL-23–IL-17 immune pathway, Trends Immunol. 27 (2006) 17–23. doi:10.1016/j.it.2005.10.003.

[17] Y. Hou, L. Zhu, H. Tian, H.-X. Sun, R. Wang, L. Zhang, Y. Zhao, IL-23-induced macrophage polarization and its pathological roles in mice with imiquimod-induced psoriasis, Protein Cell. 9 (2018) 1027–1038. doi:10.1007/s13238-018-0505-z.

[18] M.A. Eskan, R. Jotwani, T. Abe, J. Chmelar, J.H. Lim, S. Liang, P.A. Ciero, J.L. Krauss, F. Li, M. Rauner, L.C. Hofbauer, E.Y. Choi, K.J. Chung, A. Hashim, M.A. Curtis, T. Chavakis, G. Hajishengallis, The leukocyte integrin antagonist Del-1 inhibits IL-17-mediated inflammatory bone loss, Nat. Immunol. 13 (2012) 465–473. doi:10.1038/ni.2260.

[19] R. Sridharan, A.R. Cameron, D.J. Kelly, C.J. Kearney, F.J. O'Brien, Biomaterial based modulation of macrophage polarization: a review and suggested design principles, Mater. Today. 18 (2015) 313–325. doi:10.1016/j.mattod.2015.01.019.

[20] L. Chávez-Galán, M.L. Olleros, D. Vesin, I. Garcia, Much More than M1 and M2 Macrophages, There are also CD169+ and TCR+ Macrophages, Front. Immunol. 6 (2015). doi:10.3389/fimmu.2015.00263.

[21] M.E. Galarraga-Vinueza, K. Obreja, A. Ramanauskaite, R. Magini, A. Begic, R. Sader, F. Schwarz, Macrophage polarization in peri-implantitis lesions, Clin. Oral Investig. 25 (2021) 2335–2344. doi:10.1007/s00784-020-03556-2.

[22] A. Mantovani, P. Allavena, F. Marchesi, C. Garlanda, Macrophages as tools and targets in cancer therapy, Nat. Rev. Drug Discov. 21 (2022) 799–820. doi:10.1038/s41573-022-00520-5.

[23] J.C. Doloff, O. Veiseh, A.J. Vegas, H.H. Tam, S. Farah, M. Ma, J. Li, A. Bader, A. Chiu, A. Sadraei, S. Aresta-Dasilva, M. Griffin, S. Jhunjhunwala, M. Webber, S. Siebert, K. Tang, M. Chen, E. Langan, N. Dholokia, R. Thakrar, M. Qi, J. Oberholzer, D.L. Greiner, R. Langer, D.G. Anderson, Colony stimulating factor-1 receptor is a central component of the foreign body response to biomaterial implants in rodents and non-human primates, Nat. Mater. 16 (2017) 671–680. doi:10.1038/nmat4866.

[24] K.M. Hotchkiss, G.B. Reddy, S.L. Hyzy, Z. Schwartz, B.D. Boyan, R. Olivares-Navarrete, Titanium surface characteristics, including topography and wettability, alter macrophage activation, Acta Biomater. 31 (2016) 425–434. doi:10.1016/j.actbio.2015.12.003.

[25] Y. Niu, Z. Wang, Y. Shi, L. Dong, C. Wang, Modulating macrophage activities to promote endogenous bone regeneration: Biological mechanisms and engineering approaches, Bioact. Mater. 6 (2021) 244–261. doi:10.1016/j.bioactmat.2020.08.012.

[26] K. V. Holmberg, M. Abdolhosseini, Y. Li, X. Chen, S.U. Gorr, C. Aparicio, Bio-inspired stable antimicrobial peptide coatings for dental applications, Acta Biomater. 9 (2013) 8224–8231.

[27] N.G. Fischer, D.G. Moussa, E.P. Skoe, D.A. De Jong, C. Aparicio, Keratinocyte-Specific Peptide-Based Surfaces for Hemidesmosome Upregulation and Prevention of Bacterial Colonization, ACS Biomater. Sci. Eng. 6 (2020) 4929–4939. doi:10.1021/acsbiomaterials.0c00845.

[28] P. Sevilla, K. V. Vining, J. Dotor, D. Rodriguez, F.J. Gil, C. Aparicio, Surface immobilization and bioactivity of TGF-β1 inhibitor peptides for bone implant applications, J. Biomed. Mater. Res. Part B Appl. Biomater. 104 (2016) 385–394. doi:10.1002/jbm.b.33374.

[29] N.G. Fischer, E.A. Münchow, C. Tamerler, M.C. Bottino, C. Aparicio, Harnessing biomolecules for bioinspired dental biomaterials, J. Mater. Chem. B. 8 (2020) 8713–8747. doi:10.1039/D0TB01456G.

[30] C. Lamers, Overcoming the shortcomings of peptide-based therapeutics, Futur. Drug Discov. 4 (2022). doi:10.4155/fdd-2022-0005.

[31] C. Quiniou, M. Domínguez-Punaro, F. Cloutier, A. Erfani, J. Ennaciri, D. Sivanesan, M. Sanchez, G. Chognard, X. Hou, J.C. Rivera, C. Beauchamp, G. Charron, M. Vilquin, V. Kuchroo, S. Michnick, J.D. Rioux, S. Lesage, S. Chemtob, Specific targeting of the IL-23 receptor, using a novel small peptide noncompetitive antagonist, decreases the inflammatory response, Am. J. Physiol. - Regul. Integr. Comp. Physiol. 307 (2014) R1216–R1230. doi:10.1152/ajpregu.00540.2013.

[32] E.C. Wisdom, Y. Zhou, C. Chen, C. Tamerler, M.L. Snead, Mitigation of Peri-implantitis by Rational Design of Bifunctional Peptides with Antimicrobial Properties, ACS Biomater. Sci. Eng. 6 (2020) 2682–2695. doi:10.1021/acsbiomaterials.9b01213.

[33] H. Yazici, M.B. O'Neill, T. Kacar, B.R. Wilson, E.E. Oren, M. Sarikaya, C. Tamerler, Engineered Chimeric Peptides as Antimicrobial Surface Coating Agents toward Infection-Free Implants, ACS Appl. Mater. Interfaces. 8 (2016) 5070–5081. doi:10.1021/acsami.5b03697.

[34] J. Schindelin, I. Arganda-Carreras, E. Frise, V. Kaynig, M. Longair, T. Pietzsch, S. Preibisch, C. Rueden, S. Saalfeld, B. Schmid, J.-Y. Tinevez, D.J. White, V. Hartenstein, K. Eliceiri, P. Tomancak, A. Cardona, Fiji: an open-source platform for biological-image analysis, Nat. Methods. 9 (2012) 676–682. doi:10.1038/nmeth.2019.

[35] L.J. Jones, R.P. Haugland, V.L. Singer, Development and Characterization of the NanoOrange ® Protein Quantitation Assay: A Fluorescence-Based Assay of Proteins in Solution, Biotechniques. 34 (2003) 850–861. doi:10.2144/03344pt03.

[36] M.A. Dickson, W.C. Hahn, Y. Ino, V. Ronfard, J.Y. Wu, R.A. Weinberg, D.N. Louis, F.P. Li, J.G. Rheinwald, Human keratinocytes that express hTERT and also bypass a p16INK4a-enforced mechanism that limits life span become immortal yet retain normal growth and differentiation characteristics, Mol. Cell. Biol. 20 (2000) 1436–1447. doi:10.1128/MCB.20.4.1436-1447.2000.

[37] P.-H. Ding, R.P. Darveau, C.-Y. Wang, L. Jin, 3LPS-binding protein and its interactions with P. gingivalis LPS modulate pro-inflammatory response and Toll-like receptor signaling in human oral keratinocytes, PLoS One. 12 (2017) e0173223. doi:10.1371/journal.pone.0173223.

[38] D. Szklarczyk, A.L. Gable, D. Lyon, A. Junge, S. Wyder, J. Huerta-Cepas, M. Simonovic, N.T. Doncheva, J.H. Morris, P. Bork, L.J. Jensen, C. von Mering, STRING v11: protein–protein association networks with increased coverage, supporting functional discovery in genome-wide experimental datasets, Nucleic Acids Res. 47 (2019) D607–D613. doi:10.1093/nar/gky1131.

[39] A. Plesner, Increasing the yield of human mononuclear cells and low serum conditions for in vitro generation of macrophages with M-CSF, J. Immunol. Methods. 279 (2003) 287–295. doi:10.1016/S0022-1759(03)00234-5.

[40] F. Ullm, P. Riedl, A. Machado de Amorim, A. Patzschke, R. Weiß, S. Hauschildt, K. Franke, U. Anderegg, T. Pompe, 3D Scaffold-Based Macrophage Fibroblast Coculture Model Reveals IL-10 Dependence of Wound Resolution Phase, Adv. Biosyst. 4 (2020) 1900220. doi:10.1002/adbi.201900220.

[41] P.J. Murray, J.E. Allen, S.K. Biswas, E.A. Fisher, D.W. Gilroy, S. Goerdt, S. Gordon, J.A. Hamilton, L.B. Ivashkiv, T. Lawrence, M. Locati, A. Mantovani, F.O. Martinez, J.-L. Mege, D.M. Mosser, G. Natoli, J.P. Saeij, J.L. Schultze, K.A. Shirey, A. Sica, J. Suttles, I. Udalova, J.A. van Ginderachter, S.N. Vogel, T.A. Wynn, Macrophage Activation and Polarization: Nomenclature and Experimental Guidelines, Immunity. 41 (2014) 14–20. doi:10.1016/j.immuni.2014.06.008.

[42] H.E. Schroeder, M.A. Listgarten, The junctional epithelium: From strength to defense, J. Dent. Res. 82 (2003) 158–161. doi:10.1177/154405910308200302.

[43] X. Yuan, X. Pei, J. Chen, Y. Zhao, J.B. Brunski, J.A. Helms, Comparative analyses of the soft tissue interfaces around teeth and implants: Insights from a pre-clinical implant model, J. Clin. Periodontol. 48 (2021) 745–753. doi:10.1111/jcpe.13446.

[44] M.-N. Abdallah, Z. Badran, O. Ciobanu, N. Hamdan, F. Tamimi, Strategies for Optimizing the Soft Tissue Seal around Osseointegrated Implants, Adv. Healthc. Mater. 6 (2017) 1700549. doi:10.1002/adhm.201700549.

[45] M. Sartori, V. Borsari, M. Maglio, S. Brogini, L. Bragonzoni, S. Zaffagnini, M. Fini, Skin adhesion to the percutaneous component of direct bone anchored systems: systematic review on preclinical approaches and biomaterials, Biomater. Sci. 9 (2021) 7008–7023. doi:10.1039/D1BM00707F.

[46] T. Guo, K. Gulati, H. Arora, P. Han, B. Fournier, S. Ivanovski, Orchestrating soft tissue integration at the transmucosal region of titanium implants, Acta Biomater. 124 (2021) 33–49. doi:10.1016/j.actbio.2021.01.001.

[47] J.D. Hathaway-Schrader, C.M. Novince, Maintaining homeostatic control of periodontal bone tissue, Periodontol. 2000. 86 (2021) 157–187. doi:10.1111/prd.12368.

[48] R. Liu, S. Chen, P. Huang, G. Liu, P. Luo, Z. Li, Y. Xiao, Z. Chen, Z. Chen, Immunomodulation-Based Strategy for Improving Soft Tissue and Metal Implant Integration and Its Implications in the Development of Metal Soft Tissue Materials, Adv. Funct. Mater. 30 (2020) 1910672. doi:10.1002/adfm.201910672.

[49] Z. Zhuang, S. Yoshizawa-Smith, A. Glowacki, K. Maltos, C. Pacheco, M. Shehabeldin, M. Mulkeen, N. Myers, R. Chong, K. Verdelis, G.P. Garlet, S. Little, C. Sfeir, Induction of M2 Macrophages Prevents Bone Loss in Murine Periodontitis Models, J. Dent. Res. 98 (2019) 200–208. doi:10.1177/0022034518805984.

[50] S.K. Boda, C. Aparicio, Dual keratinocyte-attachment and anti-inflammatory coatings for soft tissue sealing around transmucosal oral implants, Biomater. Sci. 10 (2022) 665–677. doi:10.1039/D1BM01649K.

[51] B. Liu, Y. Jia, J. Ma, S. Wu, H. Jiang, Y. Cao, X. Sun, X. Yin, S. Yan, M. Shang, A. Mao, Tumor-associated macrophage-derived CCL20 enhances the growth and metastasis of pancreatic cancer, Acta Biochim. Biophys. Sin. (Shanghai). 48 (2016) 1067–1074. doi:10.1093/abbs/gmw101.

[52] X. Gao, J. Ge, W. Li, W. Zhou, L. Xu, D. Geng, NF-κB/let-7f-5p/IL-10 pathway involves in wear particle-induced osteolysis by inducing M1 macrophage polarization, Cell Cycle. 17 (2018) 2134–2145. doi:10.1080/15384101.2018.1515549.

[53] M.-C. Dieu-Nosjean, C. Massacrier, B. Homey, B. Vanbervliet, J.-J. Pin, A. Vicari, S. Lebecque, C. Dezutter-Dambuyant, D. Schmitt, A. Zlotnik, C. Caux, Macrophage Inflammatory Protein 3α Is Expressed at Inflamed Epithelial Surfaces and Is the Most Potent Chemokine Known in Attracting Langerhans Cell Precursors, J. Exp. Med. 192 (2000) 705–718. doi:10.1084/jem.192.5.705.

[54] I. Ghassib, Z. Chen, J. Zhu, H.-L. Wang, Use of IL-1 β, IL-6, TNF-α, and MMP-8 biomarkers to distinguish peri-implant diseases: A systematic review and meta-analysis, Clin. Implant Dent. Relat. Res. 21 (2019) 190–207. doi:10.1111/cid.12694.

[55] E. Kandaswamy, W. Sakulpaptong, X. Guo, A. Ni, H. Powell, D. Tatakis, B. Leblebicioglu, Titanium as a Possible Modifier of Inflammation Around Dental Implants, Int. J. Oral Maxillofac. Implants. 37 (2022) 381–390. doi:10.11607/jomi.9271.

[56] K.J. Maloy, The Interleukin-23 / Interleukin-17 axis in intestinal inflammation, J. Intern. Med. 263 (2008) 584–590. doi:10.1111/j.1365-2796.2008.01950.x.

[57] K. Boniface, B. Blom, Y.-J. Liu, R. de Waal Malefyt, From interleukin-23 to T-helper 17 cells: human T-helper cell differentiation revisited, Immunol. Rev. 226 (2008) 132–146. doi:10.1111/j.1600-065X.2008.00714.x.

[58] M. Seia, E. Zisman, Different roles of D-amino acids in immune phenomena, FASEB J. 11 (1997) 449–456. doi:10.1096/fasebj.11.6.9194525.

[59] B.J. Bruno, G.D. Miller, C.S. Lim, Basics and recent advances in peptide and protein drug delivery, Ther. Deliv. 4 (2013) 1443–1467. doi:10.4155/tde.13.104.

[60] X. Chen, Multi-bioactive Peptide Coatings for Dental Implants - PhD Dissertation, University of Minnesota School of Dentistry, 2014.

[61] N.G. Fischer, A.C. Kobe, J. Dai, J. He, H. Wang, J.A. Pizarek, D.A. De Jong, Z. Ye, S. Huang, C. Aparicio, Tapping basement membrane motifs: Oral junctional epithelium for surface-mediated soft tissue attachment to prevent failure of percutaneous devices, Acta Biomater. 141 (2022) 70–88. doi:10.1016/j.actbio.2021.12.030.

[62] V. V Inamdar, E. Fitzpatrick, I. Alferiev, C. Nagaswami, L.A. Spruce, H. Fazelinia, G. Bratinov, S.H. Seeholzer, R.J. Levy, I. Fishbein, S.J. Stachelek, Stability and bioactivity of pepCD47 attachment on stainless steel surfaces, Acta Biomater. 104 (2020) 231–240. doi:10.1016/j.actbio.2019.12.039.

[63] G.A. Roth, E.C. Gale, M. Alcántara-Hernández, W. Luo, E. Axpe, R. Verma, Q. Yin, A.C. Yu, H. Lopez Hernandez, C.L. Maikawa, A.A.A. Smith, M.M. Davis, B. Pulendran, J. Idoyaga, E.A. Appel, Injectable Hydrogels for Sustained Codelivery of Subunit Vaccines Enhance Humoral Immunity, ACS Cent. Sci. 6 (2020) 1800–1812. doi:10.1021/acscentsci.0c00732.

[64] K. Sadtler, A. Singh, M.T. Wolf, X. Wang, D.M. Pardoll, J.H. Elisseeff, Design, clinical translation and immunological response of biomaterials in regenerative medicine, Nat. Rev. Mater. 1 (2016) 16040. doi:10.1038/natrevmats.2016.40.

[65] J.O. Abaricia, A.H. Shah, M.N. Ruzga, R. Olivares-Navarrete, Surface characteristics on commercial dental implants differentially activate macrophages in vitro and in vivo, Clin. Oral Implants Res. 32 (2021) 487–497. doi:10.1111/clr.13717.

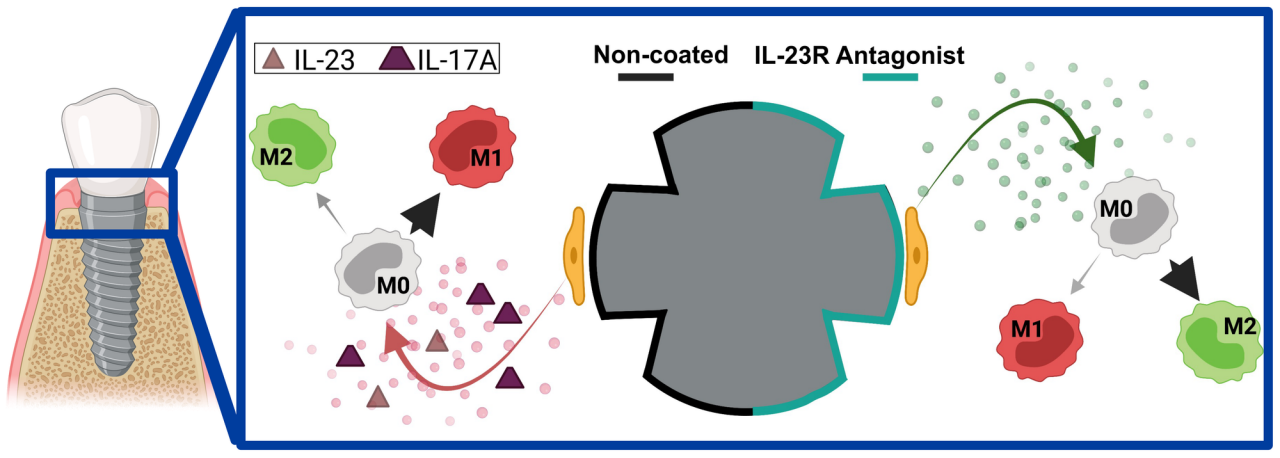
IL-23
IL-17A
Non-coated
IL-23R Antagonist
M2
M1
M0
M0
M1
M2